JOURNAL OF PROPULSION AND POWER
Vol. 23, No. 4, July–August 2007

Processing and Ignition Characteristics of Aluminum–Bismuth Trioxide Nanothermite System

Jan A. Puszynski,* Christopher J. Bulian,† and Jacek J. Swiatkiewicz‡
South Dakota School of Mines and Technology, Rapid City, South Dakota 57701

DOI: 10.2514/1.24915

During the past few years, significant progress has been made in the development of new nanoenergetic materials consisting of mixtures of metal and oxidizer nanopowders. It has been found that such reacting mixtures release energy by 2 to 3 orders of magnitude faster than similar systems consisting of micron-size reactants. In some cases, combustion-front velocities reach hundreds of meters per second. These new reacting systems find applications in both civilian and military sectors, including fast vaporization of active chemical components, fast heating of thermal batteries and main ingredients of new environmentally benign percussion primers or electric matches. This paper presents experimental results on ignition and combustion front propagation characteristics in the Al–Bi_2O_3 nanothermite system. The effect of different coatings and inhibitors of the reaction of aluminum with water in the presence and without the presence of bismuth trioxide is discussed. In addition, thermodynamic analysis of the Al–Bi_2O_3 reacting system and reaction kinetics measurements using differential scanning calorimetry are presented. Electrostatic discharge sensitivities of Al–Bi_2O_3, Al–MoO_3, and Al–Fe_2O_3 nanothermite systems were determined. It was found that all investigated nanothermite systems showed very high levels of electrostatic discharge sensitivity in the form of dry and loose powder.

I. Introduction

RECENT advances in synthesis and processing of nanopowders stimulated the exploration and development of a new class of nanoenergetic materials [1–4]. Specific examples of such materials are nanothermites or metastable interstitial composites (MIC) [5–11]. Typically, these materials consist of a mixture of aluminum and metal oxide nanopowders. Conventional thermite mixtures, which consist of micron-sized powders, have been used for many years in both military and civilian sectors because of a high level of energy release. However, the rate of energy release in such conventional thermite systems is not very fast in comparison with other energetic systems. A typical combustion front propagation velocity in a condensed phase is of the order of several centimeters to a few meters per second. Conductive heat transfer and relatively large diffusion scales are two key rate-determining steps during the condensed-phase combustion. Examples of several thermite systems, together with corresponding heat of reaction, gas generation ability, and adiabatic temperature calculated at 1 atm argon gas pressure are listed in Table 1 [12].

Several years ago, Martin et al. [5,13] demonstrated that a significant reduction of solid reactant particle sizes leads to a significant increase in the rate of energy release in thermite systems. For example, the combustion front propagation velocity has been increased by 2 to 3 orders of magnitude when the particle size of both aluminum and oxidizer was reduced to a nanosize range. Since that time, several papers have been published describing combustion front propagation and ignition characteristics in binary reacting systems consisting of nanosized aluminum and reactive oxide powders, such as MoO_3, CuO, and WO_3 [8–10]. The combined effect of a fast exothermic reaction and pressure generation, caused by product vaporization, gas expansion, and product dissociation, have led engineers to the development of lead-free percussion primers based on those nanothermite systems [14].

Molybdenum trioxide is highly reactive with aluminum due to a relatively high vapor pressure at temperatures above 800°C. Molybdenum trioxide is slightly soluble in water (1–2 grams per liter) depending on pH of the solution and it forms hydrates $MoO_3 \cdot H_2O$ or $MoO_3 \cdot 2H_2O$ [15]. The relatively low density of molybdenum trioxide ($\rho = 4,690\ \mathrm{kg/m^3}$) in comparison with bismuth trioxide, Bi_2O_3, ($\rho = 8,900\ \mathrm{kg/m^3}$), higher fuel to oxidizer stoichiometric ratio, and the possible formation of molybdenum trioxide hydrates cause a smaller volume energy output for Al–MoO_3 nanothermite. Tungsten trioxide is similar in nature to molybdenum trioxide but has a higher specific gravity. However, this oxide also easily reacts with water, forming tungstic acids. Copper oxide behaves differently than the previously mentioned molybdenum and tungsten trioxides. At elevated temperatures above 1500°C and 0.1 MPa argon pressure this oxide decomposes and releases molecular or atomic oxygen, which readily reacts with any fuel present in the mixture.

During the past couple of years, another nanothermite system, namely Al–Bi_2O_3, has been investigated [16,17]. Bismuth oxide is practically insoluble in water and with proper protection of aluminum nanoparticles the Al–Bi_2O_3 system can be mixed and processed in water slurry [18]. Bismuth oxide in water may form bismuthyl hydroxide or bismuth hydroxide, however, these compounds are 4 orders of magnitude less soluble in water as compared with MoO_3 [19].

Bismuth oxide Bi_2O_3 exists in several crystallographic forms. In Fig. 1, phase transition among different phases is shown schematically based on literature data [20].

Bismuth trioxide has four polymorphs, 1) monoclinic α form, 2) face-centered cubic δ form, 3) tetragonal β form, and 4) body centered cubic γ form. Of these polymorphs, α-$Bi_2O_3$is the only stable phase of pure Bi_2O_3 at room temperature [21]. When pure α phase is heated to about 729°C, transition to the δ-Bi_2O_3 takes place and this phase is stable only between 729°C and the melting point at 825°C [20]. Large thermal hysteresis effects are present upon cooling, and δ-Bi_2O_3 transforms to one of the two intermediate phases, which are β form (formed at 650°C) and γ form (formed at 639°C). Both γ and β phases can be obtained by controlled cooling of δ-Bi_2O_3. The γ and β forms are obtained as metastable phases at room temperature but they can be stabilized by the addition of small

---

Received 1 May 2006; accepted for publication 30 March 2007.

*Professor, Chemical and Biological Engineering Department, 501 East St. Joseph Street.

†Ph.D. Student, Chemical and Biological Engineering Department, 501 East St. Joseph Street.

‡Research Scientist, Chemical and Biological Engineering Department, 501 East St. Joseph Street.

Table 1 Thermodynamic properties of selected thermite reactions [12]

Thermite reaction	Q, cal/g	Q, cal/cm^3	Gas generation 1 atm, g gas/g mixture	T$_{ad}$, K
$2Al + Fe_2O_3 \rightarrow 2Fe + Al_2O_3$	945.4	3947	0.0784	3135
$2Al + Bi_2O_3 \rightarrow 2Bi + Al_2O_3$	505.1	3638	0.894	3319[a]
$2Al + MoO_3 \rightarrow Mo + Al_2O_3$	1124	4279	0.2473	3688[a]
$2Al + WO_3 \rightarrow W + Al_2O_3$	696.4	3801	0.1463	3253
$2Al + 3CuO \rightarrow 3Cu + Al_2O_3$	974.1	4976	0.3431	2843

[a] Values calculated in this paper.

amounts of other dopant oxides, such as Y_2O_3, MoO_3, WO_3, CaO, SrO, or V_2O_5 [22]. The powders formed by liquid phase processing or slow high temperature annealing result in the formation of a stable monoclinic α phase, whereas Bi_2O_3 powders formed by high temperature nucleation result in the formation of the tetragonal phase.

In an effort to develop a scaleable processing method, new techniques are needed, especially for effective mixing of nanopowders and consolidation of mixed energetic nanomaterials. Up to now, the majority of the published data have been focused on mixing of nanothermite binary powders in organic liquids. This approach is not recommended because most organic liquids are highly flammable and therefore such liquids should be avoided as a mixing medium for highly reactive materials, such as nanothermites. An alternative solution is processing nanopowders in water. Until a few years ago, water-based processing presented a significant problem, as aluminum nanopowder tends to react readily to form aluminum hydroxide when in contact with water vapor or liquid water [23]. Functional surface coatings, based on carboxylic acids and silanes, have been effective in protecting aluminum against liquid or vapor water for extended periods of time without a significant decrease of a reactive metal content [17,23]. Unfortunately, a hydrophobic character of formed coatings based on these surfactants prevents effective dispersion in water. Recently, other effective inhibitors of the hydration reaction, such as dicarboxylic acids or dihydrogen phosphate, have been explored [16].

Another very important constraint in the processing of energetic nanopowders is their susceptibility to electrostatic discharge. Because of the very high specific surface area of nanopowders, electrostatic charge can easily build up on such small particles. Simple agitation is sufficient to create a static buildup on that surface that will produce significant charge readings [24]. Other factors, beyond the specific properties of the components of the nanothermite system, can also affect static charge buildup as well. These include equipment, type of dispersing liquid, humidity levels of an ambient atmosphere, and effectiveness of grounding of processing containers and operators. All of these factors can also have an effect of the susceptibility of the nanoenergetic mixture to ignition by electrostatic discharge. This is one of the most important safety factors that need to be addressed before large scale processing can be implemented.

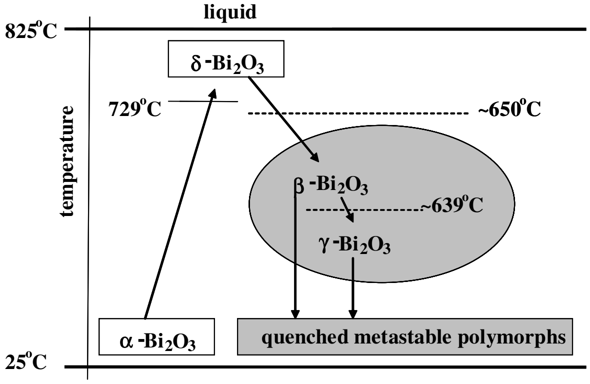

Fig. 1 Polymorphs of bismuth trioxide.

The objectives of this paper are threefold: 1) to investigate effective processing of aluminum and bismuth trioxide nanopowders in water without a noticeable deterioration of the reactants; 2) to measure ignition characteristics and kinetic parameters, such as activation energy and preexponentional factor, and 3) determine the electrostatic sensitivity of nanoenergetic materials based on aluminum and metal oxide.

II. Experimental

Aluminum and bismuth oxide nanopowders used in this study were commercially available materials. Other chemicals and coating materials were obtained from Sigma–Aldrich and Dow Corning companies as analytical reagents. The specific surface area (SSA), calculated average particle diameter, and the powder source are listed in Table 2.

Scanning electron microscope (SEM) images of examined bismuth oxide powders are shown in Fig. 2. The transmission electron microscope (TEM) images of aluminum nanopowders were published elsewhere [23]. Auger electron spectroscopy (AES) surface analysis of mixed nanopowder samples was carried out by the Evans Analytical Group using PHI 680 field emission AES nanoprobe.

Preprocessing of aluminum nanopowders was carried out according to specific chemistry of the coating reaction. The coating agents were chosen to obtain specific hydrophobic or hydrophilic surface properties of oxide passivated Al nanoparticles. Aluminum nanoparticles were coated with silanes after dispersion in anhydrous ethanol by adding partially hydrolyzed silane in a 99 wt % ethanol–water solution. The amount of silane was about 5% per total weight of solids. The solvent to solid ratio in all suspensions was equal to 5:1 by weight. This mixture was kept in ultrasonic bath for 30 min. Coating with carboxylic acids was conducted in an ethanol suspension and agitated in an ultrasonic bath for 30 min. The amount of coating material on aluminum nanopowder was 5 wt % and was the same in all tested samples. Solvent (ethanol) was removed in both procedures by evaporation during the drying of coated aluminum powders at ambient conditions. A bonded layer of phenyl-triethoxysilane on the surface of the oxide passivated aluminum nanoparticles was formed using a coating procedure that was described earlier. Its formation was confirmed by a TEM photograph [17], also shown in Fig. 3.

Water soluble inhibitors of the aluminum–water reaction such as ammonium dihydrogen phosphate or succinic acid were added directly to water during ultrasonic dispersion of the aluminum nanopowders. In this case, the aluminum powder was not dried but it was mixed with metal oxide nanopowder using the same ultrasonic equipment.

To compare kinetics of aluminum nanopowder reaction with water in the presence of various inhibitors, a pressure-tied experimental setup was used to determine the evolution of hydrogen gas as a function of time. The reaction of a sample of aluminum nanopowder suspended in water was conducted in a gas-tight closed vial connected to a pressure transducer and placed in an isothermal bath. The rate of reaction of the aluminum nanopowders in liquid water depends on the choice of inhibitor, its concentration, and temperature. Several important aspects of these studies were presented previously [20]. The measured pressure signal is proportional to the amount of evolved hydrogen. This signal was

Table 2 Specific surface area, average particle diameter, and nanopowders source

Nanopowder	SSA,[a] m^2/g	Average particle diameter,[b] nm	Source
Al (Al-40-P)[c]	45.4	41	Nanotechnologies, Inc.
Al (Al-80-P)[d]	21.7	102	Nanotechnologies, Inc.
Bi_2O_3	17.0	40	Nanophase Technologies Corp.
Bi_2O_3	2.1	321	Sigma–Aldrich
Bi_2O_3	1.62	416	Accumet Materials, Inc.
Bi_2O_3	6.24	108	Clark Manufacturing, LLC (nanosize)
Bi_2O_3	0.28	2400	Clark Manufacturing, LLC (coarse)
Fe_2O_3	45.0	26	Nanophase Technologies Corp.
MoO_3	40.0	32	Technanogy Company
CuO	31.0	31	Technanogy Company

[a] Reactant powders were characterized using BET surface area analyzer (Micromeritics Instrument Co., Model Gemini III 2375).
[b] The BET-equivalent particle diameter was calculated from a formula: $d = 6(\rho \cdot \mathrm{SSA})$, where SSA is specific surface area and ρ is density of material.
[c] Reactive aluminum content 71 wt % estimated by volumetric method.
[d] Reactive aluminum content 82 wt % estimated by volumetric method.

digitized by an analog to digital converter and sent to a computer via the RS232 link. Recorded data allowed for calculating an approximate extent of the reaction at any instant of time during experiment. The time elapsed from the moment of temperature equilibration in a vial to the onset of hydrogen evolution by a rapid pressure increase is a measure of reaction induction time. The induction time was used to evaluate initial reaction rate. The same experimental setup was used for monitoring gaseous hydrogen development during the reaction of Al and Bi_2O_3 solids suspended in liquid water.

Several methods were used to characterize the ignition and combustion characteristics of the Al–Bi_2O_3 system in comparison to other widely investigated nanoenergetic systems. Combustion front velocities were measured using an open-tray burn method [25]. The open-tray cavity (length 43 mm, width 18 mm, depth 8 mm) is fitted with two 1 mm optical ports on its base, separated by 20 mm. Fiber optic cables are connected to the ports and light signals are sent from the combustion reaction to a photodiode and recorded using an oscilloscope. A small amount of the nanoenergetic mixture, approximately 100 mg, was spread across the base of the cavity. Using a piezoelectric igniter, the mixture was spark initiated at one end of the tray. As the combustion front propagates and passes over each of the optic ports, the light signals were recorded. Combustion front velocity is calculated using the time difference between the two light signals. This method was used to investigate the Al–Bi_2O_3 system composed of Nanotechnologies Al-80-P aluminum and nanosize Clark bismuth oxide. The amount of aluminum in the system was varied from 9 to 17 wt % to determine the optimum ratio. Also tested was the effect of oleic acid protective coating on combustion front propagation.

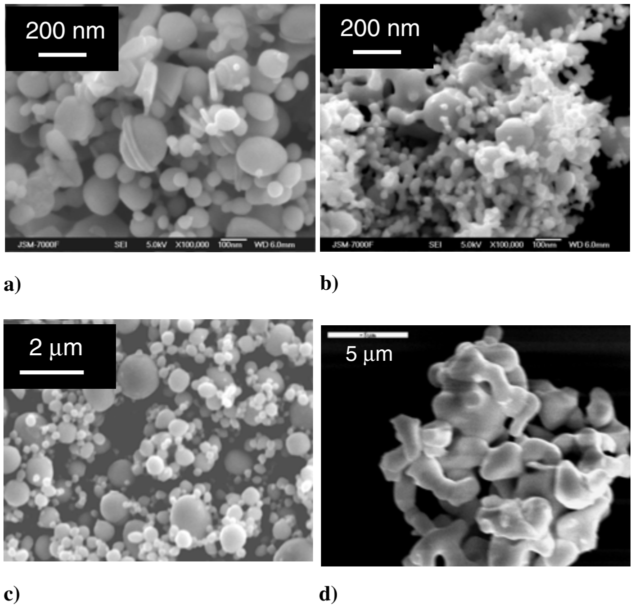

a) b)

c) d)

Fig. 2 SEM images of bismuth trioxide powders: a) Nanophase Technologies Corporation; b) Clark Manufacturing, LLC, nanosize; c) Accumet Materials, Inc.; and d) Clark Manufacturing, LLC, coarse.

Reaction kinetics and thermal ignition characteristics were investigated for nanothermite systems by differential scanning calorimetry using the instrument SDT Q600 simultaneous thermogravimetric analyzer/differential scanning calorimeter (TGA/DSC) from TA Instruments.

Other very important parameters describing the combustion behavior are ignition delay time and pressure generated by the system. In this research, a closed-volume apparatus was used for the determination of these parameters. During exothermic reaction, pressure is generated due to both expansion of gas from heating and vaporization of reaction products. A closed 25 ml volume cell was fitted with a piezoelectric pressure transducer from PCB Piezotronics. The transient pressure signal from the cell was monitored and recorded using an oscilloscope. This procedure allowed for the determination of peak reaction pressure as well as ignition delay and pressurization rate. Using uncoated Nanotechnologies Al-40-P aluminum nanopowder, CuO and MoO_3 from Technanogy and Bi_2O_3 nanosize from Clark Manufacturing, binary nanothermites systems were mixed ultrasonically in isopropyl alcohol and tested using this setup.

Another technique, based on the measurement of a recoil force, was used to determine the effect of a reactants quantity. The measurement of this force was accomplished with a recoil force load cell model ELHS-B1-1kN purchased from Entran Devices, Inc., with a response time of few microseconds. Different quantities of loose powdered energetic materials were loaded into a small primer cup, which was set on the surface of the load cell. As the material was thermally ignited, the force acted on the load cell due to gas generation and expansion and was recorded using an oscilloscope.

Electrostatic charges of nanopowders under study at various processing steps were measured using a Faraday cup and nano-Coulomb meter (Electro-Tech Systems, Inc., model 230). The initial charge on both aluminum and metal oxide powders was measured

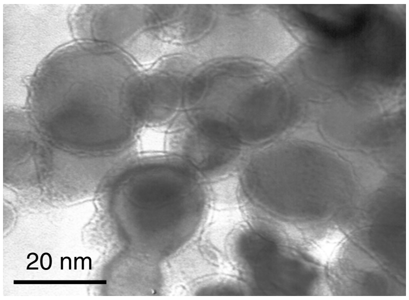

Fig. 3 Aluminum nanoparticles coated with phenyltrimethoxysilane [17].

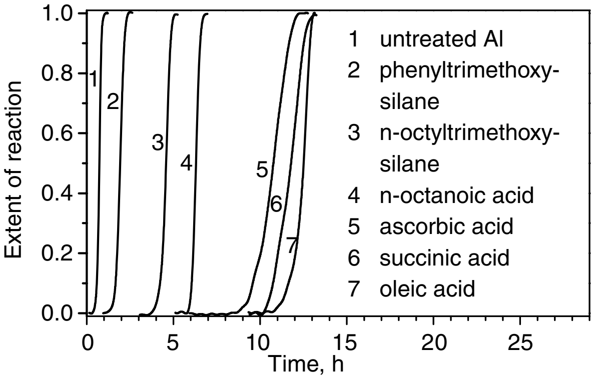

Fig. 4 Observed extent of reaction dependence on time for aluminum nanopowder reacting with water in presence of various organic inhibitors [17].

without any powder pretreatment. The effect of mass of powder tested on static charge was also investigated. To ensure consistent measurements and to mitigate the chance of accidental charging of the particles, each tested powder was stored in similar containers. The samples were weighed out into nonconducting containers and transferred to the Faraday cup for measurement.

Electrostatic discharge susceptibility was determined using LEESA (Low Energy Electrostatic Sensitivity Apparatus) [26] and an electrostatic discharge gun apparatus Model 930FTS (Electro-Tech Systems, Inc.). Using various capacitors (100, 200, 500 pF) and varying voltage from 0–25 kV, the probability of ignition via electrostatic discharge over a range of different energies can be calculated using the equation $E = V^2C/2$; where E is the ignition energy in J, V is the applied voltage in V, and C is the capacitance in F.

Several important factors affecting electrostatic discharge susceptibility of nanothermite powders were investigated including liquid processing medium, use of binders and protective coatings, and particle agglomerate size. Loose nanothermite powders were prepared in alcohol with and without protective coating on the aluminum by oleic acid. Agglomerated powder was also produced by the use of polypropylene carbonate binder in acetone. Loose powder of Al–Bi_2O_3 was also processed in liquid water in the presence of ammonium dihydrogen phosphate inhibitor. Agglomerated samples of this system were obtained after drying of the slurry, which prepared by the addition of guar gum binder during the mixing process. These samples were crushed and tested to determine the effect of the grain size on ignition energy.

III. Results and Discussion

A. Effect of Surface Coating of Aluminum Nanopowder on Its Reactivity with Water

Many surface modifiers of aluminum nanopowder are known to slowdown its reaction with water [17]. Long chain fatty acids readily react with hydroxyl groups, which are commonly present on a surface of the oxide passivated aluminum, and they form a hydrophobic layer. This layer, acting as a diffusion barrier, effectively reduces the rate of the reaction of aluminum particles with water. Other hydrophobic surface modifiers can be selected from functionalized silanes. A TEM image of aluminum nanoparticles coated with phenyltrimethoxysilane is shown in Fig. 3 [17].

To compare efficiency of reaction inhibitors, aluminum nanoparticles were treated with the same quantity of various surface modifiers and then redispersed in water before conducting the reaction in a closed-volume reactor at 48°C [17]. Dynamic pressure profiles in the reactor were recorded and later used to calculate the extent of the reaction. For comparison of initial reaction rate in the presence of various inhibitors, the induction times were evaluated from the plots in Fig. 4. The dashed lines in Fig. 4 correspond to the inhibitors with hydrophobic functional groups. Although these coatings are very effective in preventing oxidation of aluminum in water (oleic acid being the best), hydrophobic coatings generally do not allow a good dispersion of coated aluminum nanopowder in water. It was shown in these research studies [17] that dibasic acids also protect aluminum quite effectively and at the same time they enhance dispersion of such powders in water.

Calculated reaction rates obtained from the data presented in Fig. 4 are shown separately for hydrophobic and hydrophilic inhibitors in Table 3. It was found that succinic acid and ammonium phosphate were the best inhibitors for the preparation of the Al–Bi_2O_3 mixture in water.

Comparison of aluminum nanopowder oxidation rates in water as a function of the succinic acid and ammonium phosphate concentrations in the slurry, shown in Fig. 5, lead to the conclusion that ammonium phosphate is at least a 3 times more effective inhibitor than succinic acid [16]. In Fig. 6, the effect of exposure time to liquid water on the reactive aluminum content in uncoated nanopowders as well as coated ones with ammonium phosphate is shown.

The relatively fast deterioration of uncoated aluminum in water at room temperature clearly indicates that such powder cannot be used in contact with water even for a very short period of time. Contrary to that, the aluminum nanopowder dispersed in water in the presence of phosphates did show extended resistance to the hydration reaction.

It should be emphasized that the exposure to liquid water should be reduced to a minimum because this system is thermodynamically unstable. The effect of temperature on the reaction rate of aluminum nanopowder with water is shown in the form of an Arrhenius plot in Fig. 7 for uncoated and coated aluminum nanopowders with succinic acid. Effective activation energy derived from the corresponding Arrhenius plot is lower when succinic acid was applied; about 77 kJ/mol as compared with 137 kJ/mol evaluated for the reaction of uncoated aluminum with water. It should be noted that the effective activation energy, although describing accurately apparent temperature effect on the reaction rate, corresponds to all processes involved in the initial stages of aluminum nanoparticles reaction with water.

The beneficiary effect of the inhibitor is mainly due to the significant decrease of a preexponential factor (frequency factor) in the Arrhenius equation by more than 10 orders of magnitude. It might be postulated that lowering hydroxide ions concentration in the solution (a decrease of pH by the presence of succinic acid) leads to slower diffusion rates of those ions toward the surface of aluminum

Table 3 Effect of hydrophobic and hydrophilic inhibitors on rate of the aluminum reaction with water

Reaction inhibitor		Reaction rate, h^{-1}
Hydrophobic	Hydrophilic	
Trimethoxyphenyl silane[a]	——	0.67
Triethoxy-*n*-octyl silane[a]	——	0.25
n-octanoic acid[a]	——	0.17
Oleic acid[a]	——	0.088
——	Ascorbic acid[a]	0.11
——	Succinic acid[a]	0.094
——	Ammonium dihydrogen phosphate[b]	0.005
Untreated aluminum nanopowder (reference sample)		1.96

[a] 5 wt % of inhibitor was added to Al nanopowder in each experiment.

[b] 3.3 wt % of $NH_4H_2PO_4$.

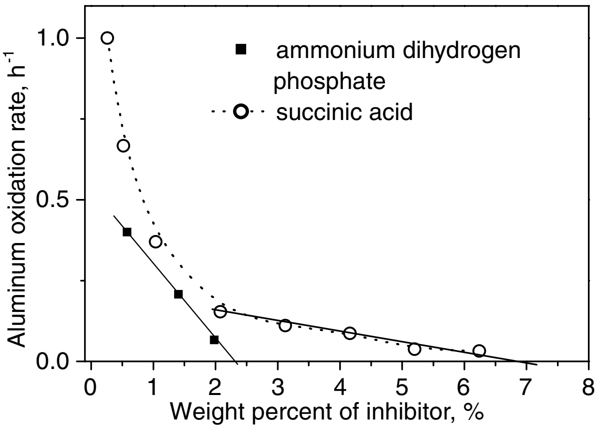

Fig. 5 Reaction rate of Al nanopowder with water as a function of inhibitor concentration at constant temperature of 48°C [16].

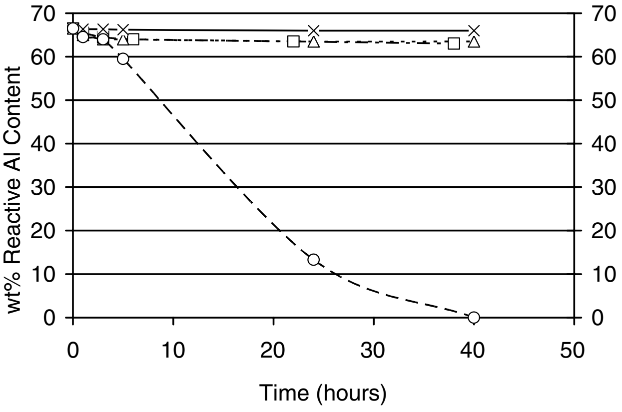

Fig. 6 The effect of exposure time to liquid water for uncoated and coated Al-40-P aluminum nanopowder at room temperature. □, 8 wt % sodium phosphate; △, 2.5 wt % succinic acid; ×, 2.5 wt % sodium dihydrogen phosphate; ○, uncoated aluminum.

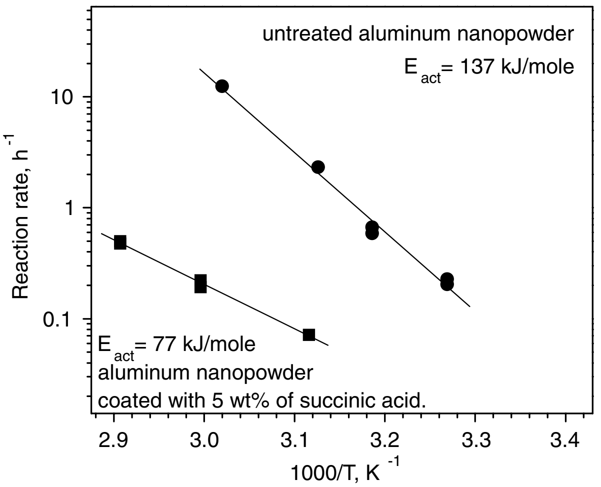

Fig. 7 Log plot of reaction rate vs inverse temperature for untreated aluminum nanopowder (circles), and aluminum nanopowder coated with 5 wt % succinic acid (squares) [17].

particles. The presence of a weak acid inhibitor facilitates control over intermediate reactions involving OH^- ions and therefore indirectly limits the reaction with aluminum nanoparticles.

The addition of bismuth trioxide into water slurry affects further the stability of aluminum nanopowder. It was found that bismuth trioxide, despite its low solubility in water, tends to contribute BiO^+ ions into the solution. These ions, despite the presence of a protective layer on aluminum nanopowder, may react slowly with aluminum.

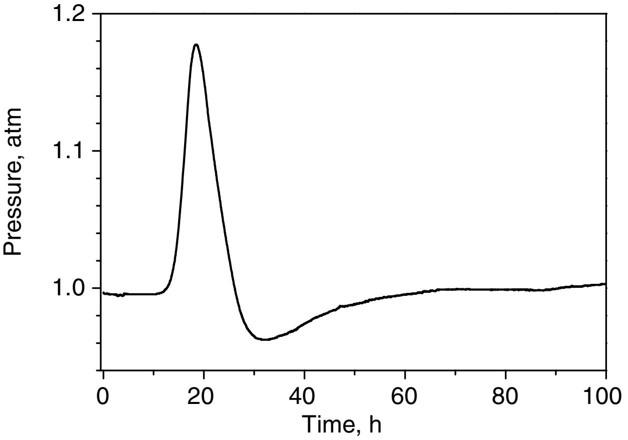

Fig. 8 Pressure change in a closed vessel during decomposition of Al–Bi_2O_3 MIC in water [16].

Decomposition of Al–Bi_2O_3 slurry in water leads to hydrogen generation, as it is observed during the reaction of aluminum nanopowder in water alone. Monitoring pressure in a closed reactor filled with the concentrated suspension of this slurry at ambient temperature reveals a slow change of pressure as shown in Fig. 8.

The reduction of BiO^+ ions at the surface of solid Al particles in water does not result in the formation of gaseous products. A plausible explanation of the observed pressure transient shown in Fig. 8 is due to the reaction of the aluminum nanoparticles in the MIC suspension with water, which generates hydrogen. This hydrogen generation leads to the increase of pressure in the reactor [16]. Subsequently, the hydrogen gas slowly reduces Bi_2O_3 dispersed in water and its partial pressure after reaching a peak decreases to zero. This observation suggests that hydrogen is only an intermediate product during the reduction of Bi_2O_3 by aluminum in water. An evident color change of the reacting mixture from dark olive to a black color at the end of the reaction indicates the reduction of Bi_2O_3 to bismuth metal. It should be noted that a reduced pressure in the gas-tight reaction chamber observed after the pressure peak is not due to ambient temperature change. Reversible sorption of the gases within a semisolid product mixture may potentially explain the origin of this event; however, this process was not explored to a sufficient extent to confirm this hypothesis.

It was also shown that the amount of the inhibitor, ammonium dihydrogen phosphate, needed in practical applications can be below 1 wt % of total solids. Under these conditions, the processing time for Al–Bi_2O_3 MIC preparation in water, including drying, should be limited to a few hours at ambient conditions. The processing time could be significantly increased if the system temperature is reduced. Protecting aluminum nanopowders against the reaction with water allows for preparing stable and concentrated aqueous suspensions. Water-based process is particularly important when safety and environmental aspects are of concern. Using water-based processing methods one can achieve a high degree of homogeneity and particle packing. This processing method was used for the preparation and direct wet loading of percussion primers, resulting in their excellent mechanical impact sensitivity performance. The performance of percussion primers is very sensitive to homogeneity of the primer mixture.

In another experiment probing efficiency of wet mixing of the nanopowders in hexane, samples of Bi_2O_3 and Al_2O_3 (alumina substituted Al metal for a safety reason) were analyzed using Auger spectroscopy imaging. The Bi and Al elemental mapping of the mixed nanopowder samples, shown in Fig. 9, reveals intermixing of the components at submicrometer scale.

B. Thermodynamics and Kinetics of Al–Bi_2O_3 Reacting System

It was previously determined that Bi_2O_3 dissociates into lower suboxide, bismuth metal, and oxygen [26]. In this study, the effect of pressure on the dissociation of bismuth oxide at elevated temperatures was calculated using the FACT and Outukumpu

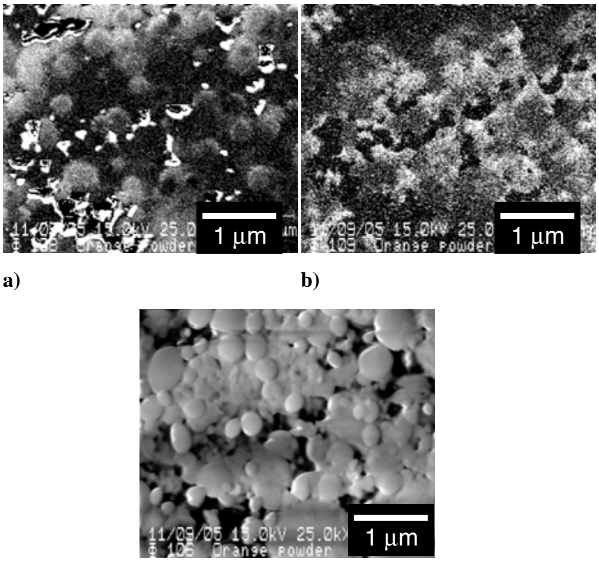

a) b)

c)

Fig. 9 AES mapping of Bi_2O_3 and Al_2O_3 nanopowder sample mixed in hexane: a) Bi elemental mapping; b) Al elemental mapping of the same area of dry sample; and c) SEM image.

HSC Chemistry 5.11 thermodynamic software packages. The equilibrium compositions of pure Bi_2O_3 and Al–Bi_2O_3 mixture in argon were calculated over a wide range of pressures ranging from 0.1 to 20 MPa and at different temperatures (up to 4000°C). Thermodynamic equilibrium data of the thermal stability of bismuth trioxide in argon at 0.1 MPa pressure shows that bismuth trioxide starts decomposing at temperatures close to 1900°C, forming BiO, Bi, and O_2 gaseous species. However, when the system pressure is higher the decomposition process takes place at significantly higher temperatures (see Fig. 10). It should be noted that different thermodynamic software packages predicted the decomposition temperature within a few hundreds degrees Kelvin.

As the temperature approaches the predicted adiabatic temperature of the reaction (~3050°C) of bismuth trioxide with aluminum, the equilibrium calculations show that most of the bismuth is present in the gas phase as Bi atoms, with the remainder as BiO vapor. Increasing the pressure over the range of 0.1–20 MPa affects both decomposition temperature and the fraction of generated gaseous products. The effect of the system temperature on equilibrium composition in condensed and gas phases at two different pressures, 1 and 200 bar, is shown in Fig. 10.

Based on the calculated equilibrium data, the adiabatic temperature was determined taking into account decomposition and vaporization of all reaction products. For each pressure, the molar fraction of products in the gas phase was also calculated. These calculations, using Outukumpu HSC thermodynamic software, were also performed for the Al–CuO–Ar and Al–MoO_3–Ar systems in an attempt to compare their equilibrium reaction behavior to Al–Bi_2O_3 system. The effect of the system pressure on the fraction of gas phase products generated under adiabatic conditions is illustrated in Fig. 11. This plot shows a significant difference in the amount of gaseous products generated by each reacting system. As expected, the Al–Bi_2O_3 system produces, in argon, the largest fraction of gaseous products in the range of examined pressures. At pressures above 0.5 MPa for Al–MoO_3–Ar and 3 MPa for Al–CuO–Ar, equilibrium data show no gas phase products present at the corresponding adiabatic temperatures. The effect of pressure on the adiabatic temperatures of all three reacting systems is shown in Fig. 12.

Figures 11 and 12 show that the adiabatic reaction temperature increases as the fraction of gaseous products decreases. In the cases of Al–MoO_3–Ar and Al–CuO–Ar the adiabatic temperatures reach a constant value (no gas products present) at 0.5 and 4 MPa, respectively.

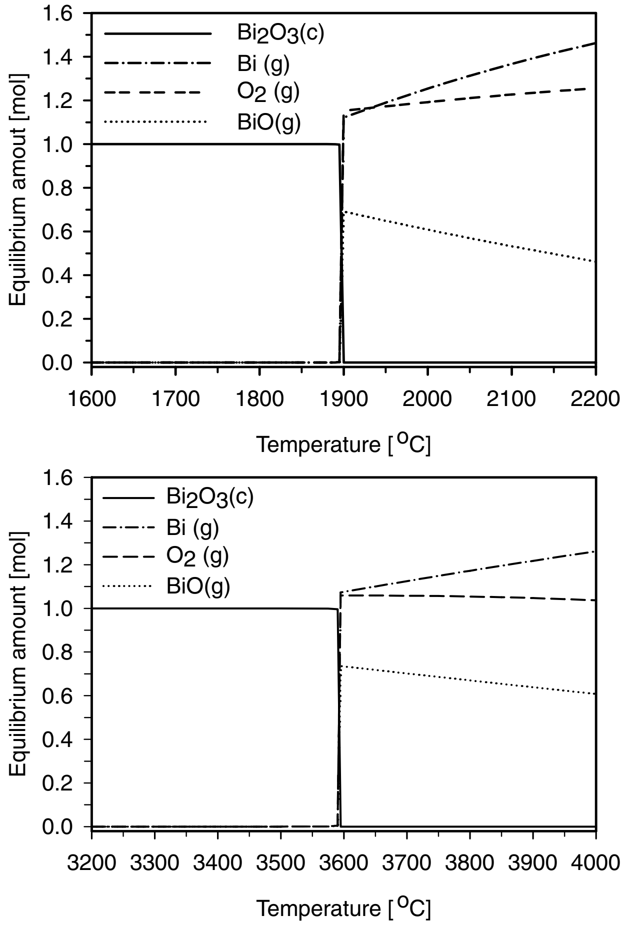

Fig. 10 Equilibrium composition plots of Bi_2O_3–Ar system at pressures of 0.1 MPa (top) and 20 MPa (bottom) calculated using FACT thermodynamic software.

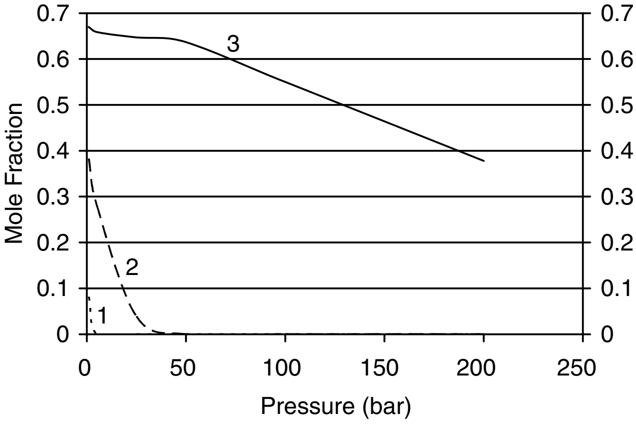

Fig. 11 Fraction of reaction products in the gas phase as a function of system pressure for 1) Al–MoO_3–Ar; 2) Al–CuO–Ar; and 3) Al–Bi_2O_3–Ar systems at their respective adiabatic temperatures of reaction.

Reaction kinetics and thermal ignition characteristics were investigated for Al–Bi_2O_3 by differential scanning calorimetry. A procedure for determining activation energy and preexponential factor was developed and outlined by the American Society of Testing and Standards, Method E 698 [27]. This test method is designed for determining Arrhenius kinetic constants for thermally unstable materials. It requires a series of DSC experiments in which the sample under investigation is heated to the point of reaction at various heating rates from 1 to 20 K/ min. For each heating rate, the peak reaction temperature is recorded. An approximate value for activation energy can be calculated using a plot of the log heat rate

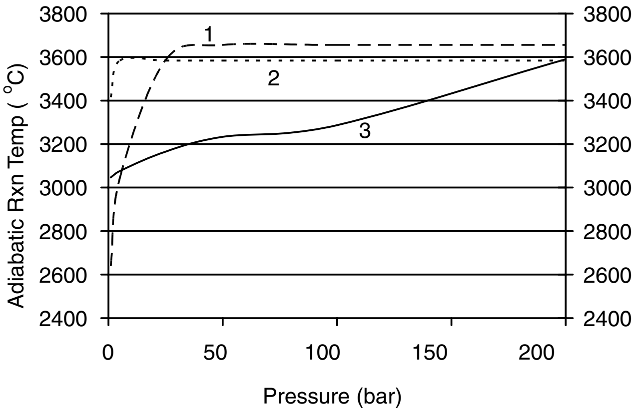

Fig. 12 Adiabatic reaction temperatures over a range of pressures for 1) Al–CuO–Ar; 2) Al–MoO_3–Ar; and 3) Al–Bi_2O_3–Ar.

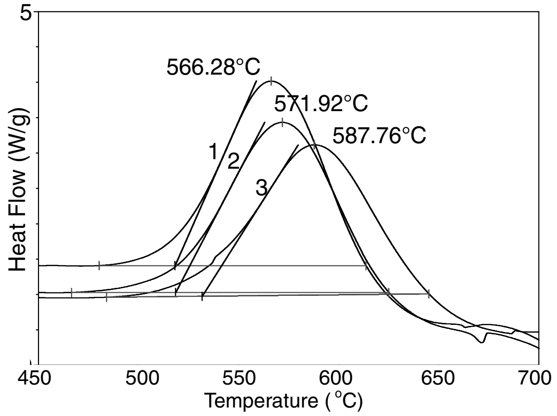

Fig. 13 DSC exothermic reaction peaks for Al–Bi_2O_3 nanothermite systems: 1) Nanophase Bi_2O_3; 2) Accumet Bi_2O_3; and 3) Clark Bi_2O_3.

versus the inverse peak reaction temperature and the following equation:

$$E \cong -2.19R[d \log \beta / d(1/T)] \tag{1}$$

where R is the gas constant, β is the heating rate in K/ min, and T is the peak reaction temperature at the corresponding heating rate. Once the value of activation energy is calculated, the preexponential factor can be determined using the equation:

$$Z = \beta E e^{E/\mathrm{RT}} / RT \tag{2}$$

This procedure was used to compare kinetic constants, E and Z, for the Al–Bi_2O_3, Al–Fe_2O_3, and Al–MoO_3 systems. The effect of coating of aluminum nanopowder with oleic acid on activation energy in the Al–Bi_2O_3 system was also determined.

It is known that a significant thermal energy barrier must be overcome in heterogeneous condensed-phase exothermic reacting systems before ignition can occur. Earlier studies showed that thermal ignition of nanoenergetic mixtures occurs at temperatures below the melting point of aluminum and below temperatures at which substantial sublimation or decomposition of corresponding oxides take place [7]. The limiting factor affecting the reaction before ignition is diffusion in a solid phase. Therefore, the rate of diffusion can be correlated to the activation energy of the system. Using differential scanning calorimetry and the American Society for Testing and Materials test method, it was confirmed that the activation energies for all three investigated nanothermite systems were indeed very high. Table 4 shows calculated activation energies, preexponential factors, and peak reaction temperatures at the heating rate of 10°C/ min.

Experimental data show that the Al–MoO_3 system has the smallest thermal energy barrier and Al–Fe_2O_3 has the highest. The presence of a protective oleic acid coating on aluminum nanopowder in the Al–Bi_2O_3 system also shows an increase in activation energy. The presence of oleic acid layer creates an addition diffusion barrier between both reactants.

The effect of bismuth oxide particle size on the peak reaction temperature was also investigated using the differential scanning calorimetry. Three different bismuth oxide powders were used, including Nanophase, Accumet, and coarse Clark powders (see Table 2). Each oxide powder was mixed in the same ratio with Nanotechnologies Al-40-P aluminum powder. The results are shown in Fig. 13.

Ignition temperature increases with the increasing average particle size of bismuth trioxide reactant. This trend can be explained by lowering the mass transfer rate caused by the reduction of effective contact area between the reactants.

C. Ignition and Combustion Front Propagation Characteristics of Al–Bi_2O_3 System

The open-tray burn test method has been commonly used for characterization of the combustion front behavior and the measurement of a front velocity in nanoenergetic systems. Previously [25], it was found that the Al–Fe_2O_3 nanothermite system has a combustion front propagation velocity of approximately 30 m/s. Combustion front propagation velocities in Al–CuO, Al–MoO_3, and Al–WO_3 nanothermites have shown over 1 order of magnitude higher values than the Al–Fe_2O_3 system [8–10]. Experimental data for Al–Bi_2O_3 reacting systems obtained using the same setup showed combustion front velocity even higher than those previously reported. Figure 14 shows combustion front propagation velocity in the Al–Bi_2O_3 system consisting of Al-80-P Nanotechnologies aluminum and nanosized Clark bismuth trioxide as a function of aluminum content in the mixture. When uncoated aluminum was used, the maximum combustion front propagation velocity was 617 m/s and the optimum ratio aluminum concentration was 14.5 wt %. When aluminum nanopowder with 5 wt % oleic acid was used instead, the combustion front velocity increased to 757 m/s for the same fuel to oxide ratio.

The unconfined open-tray test is a good screening tool but does not provide any information regarding pressure dynamics of the reaction system. Therefore, experiments in a closed-volume pressure cell were conducted. Figure 15 shows the transient pressure traces for the Al–CuO, Al–MoO_3, and Al–Bi_2O_3 reacting systems under an initial condition of 0 psig argon atmosphere [17]. Negative transients recorded before ignition is due to onset of EM noise originating from a triggering device. The results show the Al–CuO system generates the lowest peak pressure while Al–Bi_2O_3 the highest. Based on thermodynamic equilibrium data presented before, the Al–CuO system produces more gaseous products than the Al–MoO_3 system but its adiabatic temperature of reaction is almost 800°C lower. The experimental data indicate that significant pressure can still be

Table 4 Kinetic parameters for various nanoenergetic systems

Reactive system	Activation energy, kJ/mol	Preexponential factor, s^{-1}	Peak reaction temperature in °C at 10°C/ min
Al[a]–Fe_2O_3	248	1.9×10^{13}	565
Al[a]–Bi_2O_3	222	6.5×10^{11}	553
Al[a](coated)–Bi_2O_3	245	1.4×10^{13}	562
Al[a]–MoO_3	205	1.0×10^{11}	547

[a] Aluminum nanopowder: Al-40-P.

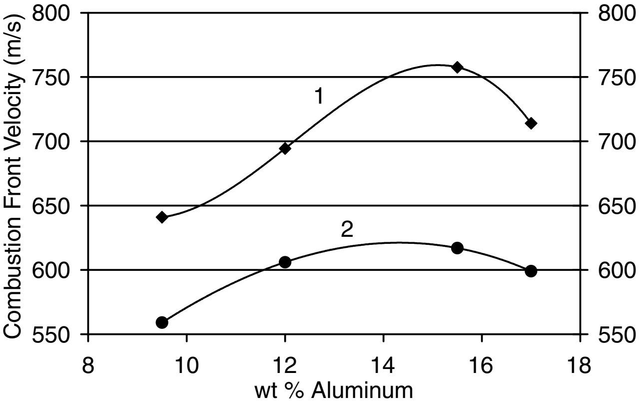

Fig. 14 Combustion front velocities in the Al–Bi_2O_3 system with 1) coated and 2) uncoated aluminum. The aluminum wt % was calculated as the ratio: mass of uncoated aluminum nanopowder per mass of uncoated aluminum and bismuth trioxide nanopowders.

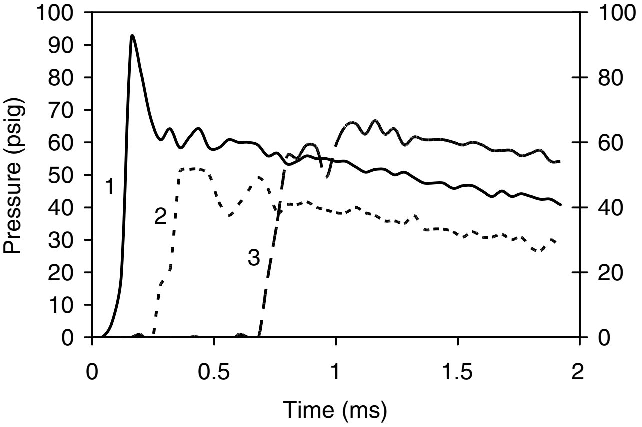

Fig. 15 Pressure traces of nanoenergetic systems in 0 psig argon initial atmosphere [17]: 1) Al–Bi_2O_3; 2) Al–CuO; and 3) Al–MoO_3.

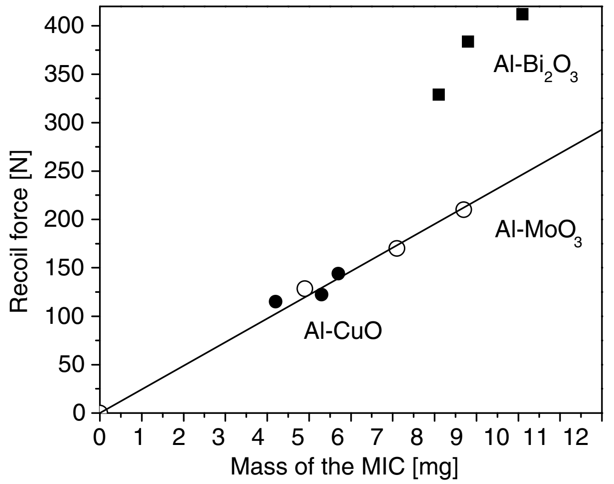

Fig. 16 Recoil force generated as a function of mass for nanoenergetic systems [17].

generated in a system in which gaseous products are not abundant if the reaction occurs fast enough, for example, Al–MoO_3.

The Al–Bi_2O_3 system, having a higher adiabatic temperature of reaction than Al–CuO, coupled with a much higher fraction of gaseous products generated than Al–MoO_3, results in the highest peak pressure of the three examined systems, when the same volume of loose reactants' mixture, were ignited.

In another experimental setup, described elsewhere [17], a reactive force was measured as a function of mass for the same three reacting systems. During these fast reactions, large localized pressure gradients are generated. Such localized pressure gradients create force on any surrounding stationary objects. Using a fast responding (μs response time) force load-cell, this effect was quantitatively measured. Experimental results showed that there was a linear dependence of force measured on mass of energetic mixture for each different system. The linear dependence was almost identical for the Al–CuO and Al–MoO_3 systems; however, the Al–Bi_2O_3 system had a greater slope and, therefore produced a greater amount of force per unit mass. These results are shown in Fig. 16.

D. Electrostatic Behavior of Nanothermite Systems

Nanoscale reactants, both fuel and oxidizer, were found to possess significant electrostatic charge even before any processing of powders. It was determined that the ability of these powders to develop surface charges is dependent not only on the high surface area of the powder, but also on the chemical nature of the material being used. Moreover, the net negative or positive charge accumulated on the powder also depends on a material contacting that powder during the frictional charging process. Therefore, only relative effects are observed even when using the same container material. In this study, glass vials were used for charging and storing nanopowders. Aluminum nanopowder, Nanotechnologies Al-80-P, has a high surface area (21.7 m^2/g) but has comparable surface charge to samples of bismuth oxide that have much lower surface areas (0.28 m^2/g). The surface charges developed on various different metal oxides, along with aluminum, are shown in Fig. 17 as a function of a sample mass. The figure also illustrates the significance of specific surface area for bismuth oxide as it relates to electrostatic charge.

Investigation of electrostatic discharge susceptibility of the Al–Bi_2O_3 system in comparison to other nanothermite systems showed a significant difference in ignition threshold. In fine powder form, all nanoenergetic mixtures are very susceptible to ignition by electrostatic discharge. Among these mixtures, however, there is a significant difference in ignition thresholds. Al–Bi_2O_3, Al–MoO_3, and Al–Fe_2O_3 systems were tested in fine powder form using a discharge capacitor of 100 pF and varying voltage to determine the minimum ignition energy. The Al–Bi_2O_3 system was found to be the most sensitive of the three examined systems, being ignited by only 0.125 μJ. The Al–MoO_3 and Al–Fe_2O_3 systems required energies of 50 μJ, and 1.25 mJ, respectively. The effect of aluminum coating on the electrostatic discharge (ESD) ignition threshold of Al–Bi_2O_3 fine powder was also investigated using both ammonium dihydrogen phosphate in water (3.3 wt % with respect to Al) and oleic acid in isopropyl alcohol (5 wt % with respect to Al). The ammonium dihydrogen phosphate was found to have no noticeable effect on the electrostatic discharge susceptibility of the system but oleic acid coating did increase the ignition threshold slightly to 4.5 μJ. The most effective method of mitigating ignition sensitivity was

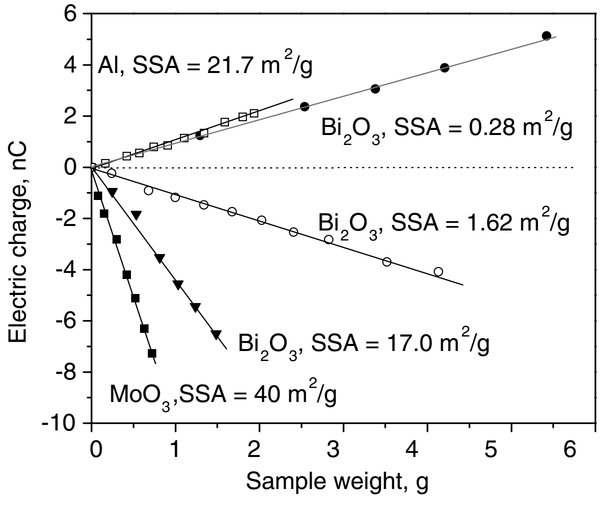

Fig. 17 Electrostatic surface charge for aluminum and metal oxide nanopowders as a function of mass [16].

determined to be mixing the aluminum and bismuth oxide in water using a guar gum as a binder. The slurry with the binder was pipetted to form small hemispherical pellets with a diameter of approximately 1 mm. In this form, the nanoenergetic mixture's sensitivity to electrostatic discharge was significantly increased to 30.2 mJ, an increase of over 4 orders of magnitude from the loose powder form. If the pellets are crushed into a finer powder form, however, they become sensitive once again, indicating that particle agglomerate size has a significant effect on the ESD sensitivity. Therefore, the processing of nanothermites should be conducted in slurries with the elimination of steps requiring handling of ultrafine dry powders.

IV. Conclusions

It was demonstrated that the dispersion of aluminum nanopowders and their mixing with bismuth trioxide oxidizer can be accomplished in liquid water without a noticeable deterioration of both reactants. Ammonium dihydrogen phosphate has been found to be a very effective inhibitor of the reaction of aluminum nanopowder with water in slurries containing both aluminum and bismuth trioxide nanopowders.

Both thermodynamic calculations and experiments conducted under unconfined and confined conditions revealed that the Al–Bi_2O_3 system is more reactive than other examined nanothermite mixtures and can likely contribute a comparatively larger fraction of gaseous products generated during the combustion.

Kinetics parameters for various heterogeneous exothermic reactions between aluminum and metal oxides nanopowders were determined by the DSC technique. It was found that the activation energies for Al–Fe_2O_3, Al–MoO_3, Al(uncoated)–Bi_2O_3, and Al (5 wt% oleic acid)–Bi_2O_3 are 248 kJ/mol, 205 kJ/mol, 222 kJ/mol, and 245 kJ/mol, respectively.

The electrostatic charge buildup on dry nanopowder is affected by many handling factors, therefore mixing and processing of nanoenergetic materials should be done with the elimination or minimization of all steps involving dry-powder processing.

Acknowledgments

The authors gratefully acknowledge the financial support from the U.S. Army Research Office (Grant No. DAAD19-01-1-0503 and Grant No. W911NF-05-1-0310) and the U.S. Naval Surface Warfare Center, Indian Head (Contract No. N00174-05-M-0141).

References

[1] Dorsett, H. E., Brousseau, P., and Cliff, H. E., "The Influence of Ultrafine Aluminum upon Explosives Detonation," *Proceedings of the 28th International Pyrotechnics Symposium*, IPSUSA Seminars, Inc., Littleton, CO, 2001, pp. 239–244.

[2] Pivkina, A., Frolov, Y., Zavyalov, S., Ivanov, D., Schoonman, J., Streletskii, A., and Butyagin, P., "Ultra-Fine and Nanosized Oxidizers and Metals: Thermal Ignition Properties and Use in High Energetic Compositions," *Proceedings of the 31st International Pyrotechnics Seminar*, IPSUSA Seminars, Inc., Littleton, CO, 2004, pp. 285–298.

[3] Miziolek, A. W., "Nanoenergetics: An Emerging Technology Area of National Importance," *Amptiac Quarterly*, Vol. 6, No. 1, 2002, pp. 43–48.

[4] Mench, M. M., Kuo, K. K., Yeh, C. L., and Lu, Y. C., "Comparison of Thermal Behavior of Regular and Ultra-Fine Aluminum Powders (Alex) Made From Plasma Explosion Process," *Combustion Science and Technology*, Vol. 135, Nos. 1–6, 1998, pp. 269–292.

[5] Martin, J. A., Murray, A. S., Hollander, M. G., and Kung, H., "Metastable Interstitial Composites," *Warhead Technology*, Vol. 1, June 1997, pp. 141–153.

[6] Son, S. F., Busse, J. R., Asay, B. W., Peterson, P. D., Mang, J. T., Bockmon, B., and Pantoya, M. L., "Propagation Studies of Metastable Intermolecular Composites (MIC)," *Proceedings of the 29th International Pyrotechnics Seminar*, IPSUSA Seminars, Inc., Littleton, CO, 2002, pp. 203–212.

[7] Bulian, C. J., Kerr, T. T., and Puszynski, J. A., "Ignition Studies of Aluminum and Metal Oxide Nanopowders," *Proceedings of the 31st International Pyrotechnics Seminar*, IPSUSA Seminars, Inc., Littleton, CO, 2004, pp. 327–338.

[8] Son, S. F., Hiskey, H. L., Asay, B. W., Busse, J. R., Jorgensen, B. S., Bockmon, B., and Pantoya, M., "Reaction Propagation Physics of Al/MoO_3 Nanocomposite Thermites," *The Twenty-Eighth International Pyrotechnics Seminar*, IPSUSA Seminars, Inc., Littleton, CO, 2001, pp. 833–842.

[9] Somasundaram, V., Bulian, C. J., and Puszynski, J. A., "Investigation of Al–CuO Nanocomposite Reacting Systems," *Proceedings of EUROPYRO 2003*, Vol. 2, Association Francaise de Pyrotechnie, La-Ferte-Saint-Aubin, 2003, pp. 536–541.

[10] Perry, W. L., Smith, B. L., Bulian, C. J., Busse, J. R., Macomber, C. S., Dye, R. C., and Son, S. F., "Nano-scale Tungsten Oxides for Metastable Intermolecular Composites," *Propellants, Explosives, Pyrotechnics*, Vol. 29, No. 2, 2004, pp. 106–111.

[11] Plantier, K. B., Pantoya, M. L., and Gash, "Combustion Wave Speeds of Nanocomposites Al/Fe_2O_3: The Effects of Fe_2O_3 Particle Synthesis Technique," *Combustion and Flame*, Vol. 140, No. 4, 2005, pp. 299–309.

[12] Fischer, S. H., and Grubelich, M. C., "Theoretical Energy Release of Thermites, Intermetallics, and Combustable Metals," *Proceedings of the 24th International Pyrotechnics Seminar*, IPSUSA Seminars, Inc., Littleton, CO, 1998.

[13] Aumann, C. E., Skofronick, G. L., and Martin, J. A., "Oxidation Behavior of Aluminum Nanopowders," *Journal of Vacuum Science and Technology B*, Vol. 13, No. 3, 1995, pp. 1178–1183.

[14] Puszynski, J. A., Swiatkiewicz, J. J., and Bichay, M. M., South Dakota School of Mines and Technology, Rapid City, SD, and U.S. Navy, U.S. Patent Application for "Nanoenergetic Materials Based on Aluminum and Bismuth Oxide," Docket No. 11/000,678, filed 30 Nov. 2004.

[15] Killeffer, D. H., and Linz, A., *Molybdenum Compounds: Their Chemistry and Technology*, Interscience, New York, 1952.

[16] Puszynski, J. A., Bulian, C. J., Swiatkiewicz, J. J., and Bichay, M. M., "Challenges in Processing of Aluminum and Metal Oxide Nanopowders and Water," *Proceedings of the 5th World Congress on Particle Technology*, American Institute of Chemical Engineers, New York, NY, 2006; Paper No. 247D.

[17] Puszynski, J. A., Bulian, C. J., and Swiatkiewicz, J. J., "The Effect of Nanopowder Attributes on Reaction Mechanism and Ignition Sensitivity of Nanothermites," *Materials Research Society Symposia Proceedings*, Vol. 896, 2006, pp. 147–158.

[18] Puszynski, J. A., Swiatkiewicz, J. J., and Bichay, M. M., Innovative Materials and Processes, LLC, Rapid City, SD, and U.S. Navy, U.S. Patent Application for "Wet Processing and Loading of Percussion Primers Based on Metastable Nanoenergetic Composites," Docket No. 20,060,113,014, filed 1 June 2006.

[19] *CRC Handbook of Chemistry and Physics*, 72nd ed., edited by R. C. Weast, CRC Press, Boston, 1992.

[20] Turkoglu, O., Soylak, M., and Belenli, I., "Synthesis and Characterization of β type Solution in the Binary System of Bi_2O_3–Eu_2O_3," *Bulletin of Materials Science*, Vol. 25, No. 7, Dec. 2002, pp. 583–588.

[21] Oniyama, E., and Wahleck, P. G., "Phase Equilibria in the Bismuth–Oxygen System," *Journal of Physical Chemistry*, Vol. B102, No. 22, 1998, pp. 4418–4425.

[22] Ling, C. D., Withers, R. L., Schmid, S., and Thompson, J. G., "A Review of Bismuth-Rich Binary Oxides in the Systems Bi_2O_3–Nb_2O_5, Bi_2O_3–Ta_2O_5, Bi_2O_3–MoO_3, and Bi_2O_3–WO_3," *Journal of Solid State Chemistry*, Vol. 137, No. 1, 1998, pp. 42–61.

[23] Puszynski, J. A., "Reactivity of Nanosize Aluminum with Metal Oxides and Water Vapor," *Materials Research Society Symposia Proceedings*, Vol. 800, 2004, p. AA6.4.1.

[24] Noras, M. A., "Measurement of Flowing Charges with an Electrostatic Voltmeter," *Proceedings of the 39th Annual Meeting of the IEEE Industry Applications Society*, IEEE Publications, Piscataway, NY, 2004, pp. 2714–2716.

[25] Valliappan, S., Swiatkiewicz, J. J., and Puszynski, J. A., "Reactivity of Aluminum Nanopowders with Metal Oxides," *Powder Technology*, Vol. 156, 2005, pp. 164–169.

[26] Carlson, R. S., and Wood, R. L., "Development and Application of LEESA (Low Energy Electrostatic Sensitivity Apparatus)," *Proceedings of the Fifteenth International Pyrotechnic Seminar*, IPSUSA Seminars, Inc., Littleton, CO, 1990, pp. 161–180.

[27] American Society for Testing and Materials, "Standard Test Method for Arrhenius Kinetic Constants for Thermally Unstable Materials," *Designation*, Vol. E698-79, 1984, pp. 624–631.

S. Son
Associate Editor